Widely-tunable single-mode interband cascade lasers based on V-coupled cavities and dependence on design parameters

Zhanyi Wang [1], Jingli Gong [1], Jian-Jun He [1,a)], Lu Li [2], Rui Q. Yang [2,a)] and James A. Gupta [3]

[1]State Key Laboratory of Modern Optical Instrumentation, College of Optical Science and Engineering, Zhejiang University, Hangzhou, China 310027

[2]School of Electrical & Computer Engineering, University of Oklahoma (OU), Norman, OK, USA 73019

[3]National Research Council of Canada, Ottawa, Ontario, Canada K1A 0R6

[a)] Electronic mail: jjhe@zju.edu.cn, Rui.q.Yang@ou.edu

We report an investigation of V-coupled cavity interband cascade (IC) lasers (ICLs) emitting in the 3-μm wavelength range, employing various waveguide structures and coupler sizes. Type-II ICL devices with double-ridge waveguides exhibited wide tuning ranges exceeding 153 nm. Type-I ICL devices with deep-etched waveguides achieved single-mode emission with wavelength tunable over 100 nm at relatively high temperatures up to 250 K. All devices exhibited side mode suppression ratio higher than 30 dB. By comparing the performance for all devices with different sizes and configurations, a good tolerance against the structural parameter variations of the V-coupled cavity laser (VCCL) design is demonstrated, validating the advantages of the VCCL to achieve single-mode emission with a wide tunability.

I. INTRODUCTION

Mid-infrared (IR) semiconductor lasers have many applications in chemical sensing, food safety, environmental and greenhouse gas monitoring, detection of pipeline leaks and explosives, medical diagnostics, and industrial process control. Interband cascade lasers (ICLs), which were first proposed in 1994[1] and initially demonstrated experimentally in 1997[2], have become important semiconductor mid-infrared light sources in the wavelength range from 3-6 μm[3-6]. Recently, the wavelength coverage of ICLs has been extended beyond 14 μm[7]. Tunable single-mode lasers with high spectral purity are required in high sensitivity applications. Lithographically-defined distributed feedback (DFB) gratings are one of the commonly used solutions for achieving single-mode lasers[8-12]. A commercially available DFB ICL demonstrated a tuning range of 10 cm^{-1} near 3.3 μm with the injected current varying from 0.45 A to 0.76 A, at 15 ℃ to 35 ℃, while the maximum continuous-wave (CW) output power decreased from 22 mW to around 8 mW with the increased temperature[12]. Due to the limited tuning range of DFB lasers, the grating period and the fabrication process need to be well-controlled so that the laser wavelength matches the desired operating wavelength. Accurate control of the grating period and the fabrication process is costly, however, and reduces the fabrication yield. Introducing external cavity (EC) components for mode selection and tuning is also widely used in single-mode lasers[13-14]. An external cavity ICL was reported by Alpes Lasers with a wide tuning range over 360 nm by adjusting the external grating angle[14]. However, the discrete components make the system bulky and costly, and the integration is challenging due to stability requirements.

Alternatively, single-mode emission with a wide tuning range can be achieved in the V-coupled cavity laser[15] (VCCL) configuration, which was first demonstrated in InGaAsP/InP material systems with a high side mode suppression ratio (SMSR) over 38 dB[16]. The VCCL offers an inexpensive and monolithically-integrated solution for tunable single-mode lasing, with no need for grating fabrication or regrowth steps. Hence, the combination of ICLs with VCCL configuration may produce a more viable tunable single-mode mid-IR light source that can meet practical application needs. Following our initial demonstration of a single-mode V-coupled cavity ICL at low temperatures (≤120 K) with a 60-nm tuning range near 2.9 μm reported in 2020[17], we recently reported a mid-IR tunable single-mode V-coupled cavity ICL near 3.4 μm with a tuning range exceeding 100 nm and a maximum SMSR as high as 35.7 dB[18]. Furthermore, using a type-I ICL wafer, we demonstrated tunable single-mode VCCLs near 3 μm with a total tuning range of around 210 nm over a wide temperature range and CW operation at temperatures up to 240 K[19]. These recent results suggest that tunable single-mode ICLs based on the VCCL configuration have significant advantages over conventional DFB lasers and are expected to be developed further for practical applications.

In this work, we report a comparative study of several tunable single-mode V-coupled cavity ICLs made from two different wafers, which have different waveguide structures and coupler parameters. All these ICLs exhibited single-mode operation with tuning range exceeding 100 nm and the maximum side-mode-suppression-ratio (SMSR) larger than 30 dB, indicating good tolerances of device performance against structural parameter variations. These results further validate the benefits of VCCL configuration for achieving wide-tunable single-mode operation.

II. EXPERIMENTAL

A. ICL Materials

ICLs are constructed from the nearly lattice-matched InAs/GaSb/AlSb III-V material system. Due to a large conduction-band offset and type-II band-edge alignment in this Sb-based system, excellent carrier confinement and wide wavelength coverage can be achieved in ICLs[20-22]. In this work, both a type-II ICL wafer and a type-I ICL wafer were used. The type-II ICL is based on type-II W-quantum well (QW)[5,21] active region where electron and hole wavefunctions are located mainly in different layers in contrast to the type-I ICLs[23-25] where electrons and holes are primarily confined in the same well layer. The type-II ICL wafer used in this work is the same as that in reference 18, which comprises 12 cascade stages, the InAs/AlSb superlattice (SL) cladding layers, and the InAs contact layer as shown in Fig. 1(a). A piece of this type-II ICL wafer was previously processed using wet etching into 15-μm-wide ridge laser devices that lased in pulsed mode at temperatures up to 300 K and more details were given in Ref. 18. The type-I ICL wafer used in this work is similar to the ICL structure in Ref. 24 and composed of 6 cascade stages based on a $Ga_{0.45}In_{0.55}As_{0.22}Sb_{0.78}$ QW active region, GaSb separate confinement layers (SCLs) and InAs/AlSb SL cladding layers, as shown in Fig. 1(b), with an InAs contact layer on the top, which was the same as that (V1080) in Ref. 19. A piece of this type-I ICL wafer was also previously processed into broad-area (BA) devices that lased in CW mode to 240 K and to 365 K in pulsed mode as described in Ref. 19, which had better device performance with lower threshold current density than that for devices made from the type-II ICL wafer used in this work. However, it should be noted that both wafers do not represent state-of-the-art ICL structures in terms of device performance, and they were used to prove the concept and advantages of the VCCL configuration in

mid-IR wavelength region. The state-of-the-art type-II ICLs have already been demonstrated in CW mode at temperatures above 300 K (room temperature) in the 3-6 μm region[3-6], which have substantially better device performance than the two wafers used in this work. Hence, significantly improved device performance is expected at high temperatures when the state-of-the-art ICL wafers are used after advantages of the VCCL configuration are demonstrated using old ICL wafers.

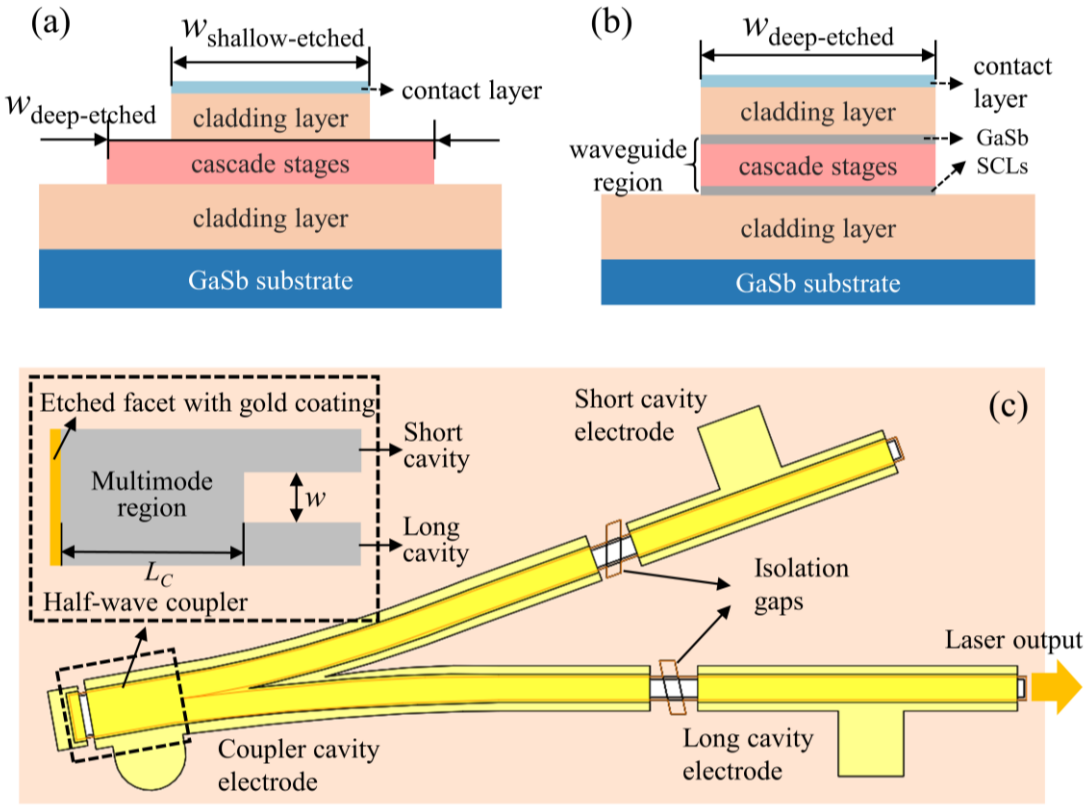

FIG. 1. The schematic drawing of the cross-sectional view of (a) the double-ridge waveguide based on type-II ICL wafer and (b) the deep-etched waveguide based on type-I ICL wafer. (c) The schematic drawing of a V-coupled cavity laser.

B. Waveguide Structure and VCCL Configuration

The VCCL is simple in structure, reliable in operation, and small in size without complex grating fabrication or multiple epitaxial growths. The schematic drawing of a monolithically integrated VCCL is shown in Fig. 1(c), in which two

Fabry-Perot (FP) waveguide cavities of different lengths are joined with a half-wave coupler. In an ideal half-wave coupler, the cross-coupling coefficient C_x has a relative phase of π with respect to the bar-coupling coefficient C_b, and the two output ports obtain the synchronous power transfer functions[15]. We define the normalized cross-coupling coefficient $\chi = C_x^2/(C_x^2 + C_b^2)$ as an important parameter for optimizing the design of the coupler. According to the description of the working principle in Ref. 15, the threshold gain difference between the longitudinal modes with the lowest and second lowest thresholds is a function of the normalized cross-coupling coefficient χ. In this case, the dimensional parameters of the half-wave coupler, the length of the multimode region (L_C) and the gap of the two waveguides (w), need to be chosen to achieve the targeted value of χ (that corresponds to the peak of the threshold gain difference) and the relative phase (near 180°) to maximize SMSR of the lasing modes. By scanning in the finite difference time domain (FDTD) analysis, we usually determine the values of the two parameters within an appropriate range in order to get the value of χ close to theoretical optima (equal to 0.02 for devices in this work) and the relative phase close to π.

The wide tunability of VCCLs can be achieved through the Vernier effect due to the slight difference in the lengths of two FP cavities, as described in Ref. 15. The resonance frequency intervals of FP cavities are determined by $\Delta f = c/\left(2n_g L\right)$, where c is the light velocity in vacuum, n_g is the effective refractive index of the waveguide, and L is the length of the cavity. The frequency interval of the short cavity (the current of which is usually fixed during current tuning) defines the channel spacing of the device. Moreover, the length difference is related to the amplification factor of the Vernier effect and free spectral range by differentiating the frequency interval between the two cavities. The smaller the length difference, the larger the Vernier

amplification factor and the free spectral range. The lengths of the two cavities in VCCLs need to be sufficiently long so that the threshold current density is low enough for good ICL performance. On the other hand, the SMSR decreases with increasing cavity lengths and decreasing length difference, due to smaller mode interval and broader filtering function, respectively. Therefore, the cavity lengths and the length difference need to be appropriately chosen with considerations of the above trade-offs.

In the V-coupled cavity lasers, the wavelength can be tuned by adjusting the operating temperature and the currents of three electrodes as shown in Fig. 1(c). At a fixed temperature, the long cavity electrode is used to select the wavelength channel by changing the injection current I_L. The currents of the coupler electrode I_C and short cavity electrode I_S are usually fixed to provide fixed gain for lasing and can be manually adjusted to obtain auxiliary tuning and improve the SMSR of the channel. In addition, changing the temperature can shift the gain spectrum to extend the tuning range.

C. Device Fabrication

A deep etching through the cascade stages is usually employed in the ICLs to ensure uniform current injection over every cascade stage, as shown in Fig. 1(b). Devices with deep-etched waveguide configurations were made on the type-I ICL wafer with 8-μm-wide ridge waveguides. The double-ridge waveguide structures, in which the widths of the shallow waveguide and deep waveguide are different, as shown in Fig. 1(a), can avoid substantial current leakage through side walls and light scattering loss caused by the narrow deep-etched ridge[18,26]. By employing this double-ridge waveguide structures, devices were made from the type-II ICL wafer with the widths of 8 μm and 10 μm for the shallow-etched waveguide. The fabrication process

for devices with two different waveguide configurations was the same, except that devices with double-ridge waveguides require an extra etching step.

The isolation gaps were first defined by wet etching down through the contact layer. Before the ridge etching, a 150 nm thick Ti-Pt-Au layer was deposited to avoid the destruction of the contact layer during the etching of the top via window. A 550-nm-thick SiO_2 film was deposited using plasma-enhanced chemical vapor deposition for passivation and electrical isolation. After the hard mask was opened using a fluorine-based dry etch, the waveguide pattern was transferred to the ICL sample using a BCl_3-Ar dry etch.

For deep-etched devices, the waveguide was etched down through the waveguide region of the type-I ICL wafer to the bottom cladding layer to limit the lateral current spreading. The three etched facets of waveguides were also formed in this etching step and served as cavity mirrors. For double-ridge devices, an additional etching step for the shallow-etched waveguide was necessary before etching the deep-etched ridge for lateral confinement of current. The depth of the shallow-etching was controlled by manually setting the etching time and should stop at the interface between the upper cladding layer and cascade stages. Then a deep-etching was performed down through the cascade stages. Afterward, an extra deep etching step was executed to form the end facets of the waveguides after the formation of the waveguide ridges.

Finally, a contact window was opened on the top of waveguides and a Ti-Pt-Au layer of electrode pads was sputtered on the top of chips via a lift-off process. The GaSb substrate was then thinned down to 150 μm and polished. After the formation of Ti-Pt-Au contact on the backside, the chips were rapidly annealed at 350 °C for 1 min

and then cleaved into laser bars. The laser bars were mounted epi-side up on copper heat sinks through In-Au alloying for characterization.

III. RESULTS AND DISCUSSION

A. Electrical and optical characteristics

Each device was mounted epitaxial-side-up on a copper heat sink attached to a temperature-controlled cryostat. An integrating sphere photodiode HgCdTe (MCT) power sensor from Thorlabs was used to measure the output optical power of one facet through the optical CaF_2 cryostat window, and the optical power is corrected by ~10% transmission loss. The measured output power of the devices was conservative because the beam divergence loss was not taken into account. The emission spectra were measured by a Bruker Vertex 70 Fourier transform IR (FTIR) spectrometer with a spectral resolution of 0.3 cm^{-1} (~0.35 nm at 3.4 μm). The structural parameters of the different ICL devices in this work and previous work are listed in Table I. The lengths of the short FP cavities of the type-I ICL devices are 1000 μm. For type-II ICL devices, the lengths of short FP cavities are around 883 μm. The long cavities for all devices are 5% longer than the short cavities.

Figure 2 shows the voltage-current and power-current characteristics of the laser devices in CW operation. The output power was measured for the beam from the facet of the long cavity. In the experiment, with fixed long cavity current and short cavity current, the output power increased with the coupler current I_C and eventually saturated. The type-II ICLs lased at temperatures up to 120 K with higher threshold current densities. Device II-A with a shallow etched waveguide width of 8 μm delivered an output power of 5 mW at 80 K. The maximum output power of device II-B was 3.6 mW at 80 K, lower than device II-A, which may be caused by the narrower

deep-etched waveguide with a higher threshold current density as shown in Fig. 3. Compared with the above type-II ICLs, the devices based on type-I ICL wafer were able to operate at much higher temperatures because of the significantly lower threshold current densities as shown in Fig. 3. Device I-C with an 8-μm-wide deep etched waveguide was able to deliver an output power of 9.6 mW at 150 K and still around 5 mW at 210 K, with single-mode tunable wavelength. As for device I-D, with a similar structure to device I-C, its output power was slightly lower at low temperatures, but it lased at higher temperatures up to 250 K. The output power characteristics of 8-μm-wide deep-etched type-I ICLs in this work are similar to the earlier results of device B in reference 19 with the same waveguide structure.

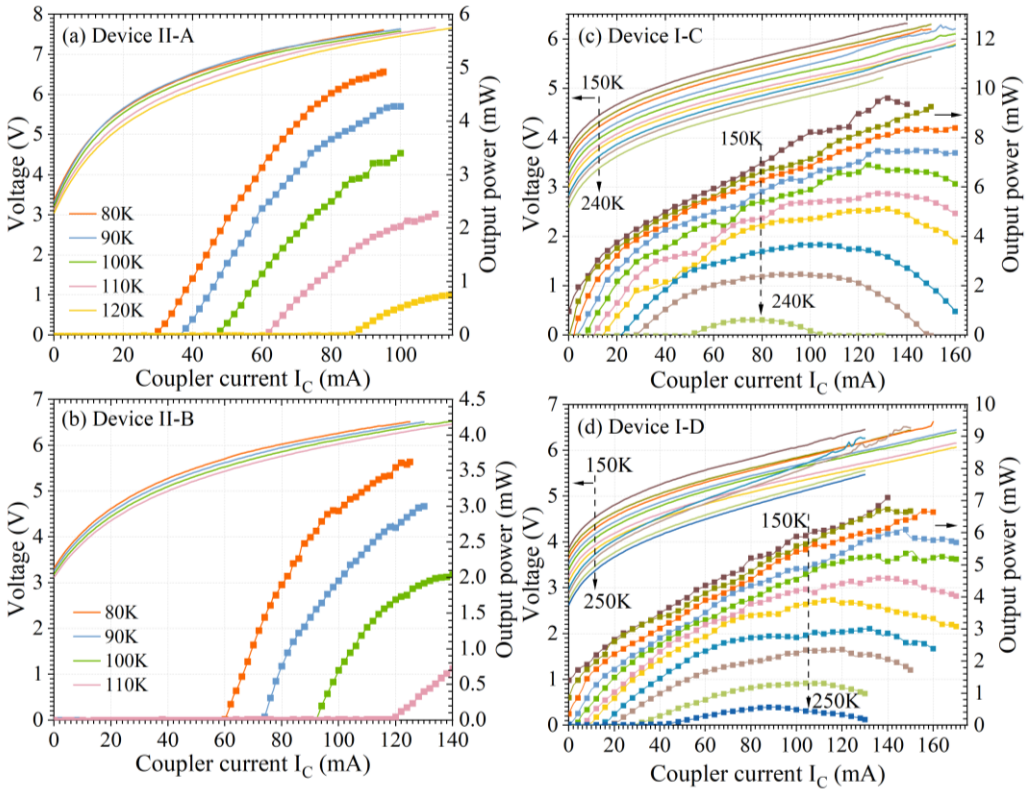

FIG. 2. Electrical and optical characteristics of IC VCCLs at different temperatures. Devices (a) II-A and (b) II-B: the long cavity current is 40 mA and the short cavity current is 30 mA; devices (c) I-C and (d) I-D: the long cavity current and the short cavity current are both 30 mA.

The temperature-dependent threshold current densities for the ridge lasers operated in CW mode are summarized in Figure 3, along with the devices reported

previously. For type-I ICL devices with 8-μm-wide deeply etched waveguide structure, the value of the threshold current density J_{th} was similar and small. The total threshold current density of device I-D was about 48.7 A/cm^2 at 80 K and increased to 390 A/cm^2 at 240 K and 540 A/cm^2 at 250 K. As for type-II ICL devices with double-ridge waveguide structure, the values of J_{th} were higher than those of the deeply-etched devices. The J_{th} of device II-A was 240, 256, 280, 314 and 372 A/cm^2 at 80, 90, 100, 110 and 120 K, respectively, which is approximately the same order of magnitude as that of the device on the same wafer in Ref. 18. Device II-B had values of J_{th} more than twice the values of device II-A, which may be caused by more leakage current through side walls with the narrower deep-etched waveguide. The threshold current densities of devices based on the type-I ICL wafer are substantially lower than those of the type-II ICLs with double-ridge waveguides, which is consistent with the better performance characteristics of type-I ICL BA devices described in section II.A. Because of the lower J_{th}, the type-I ICL devices can operate at higher temperatures. In theory, devices employing double-ridge structures should have better performance with lower threshold current density and higher operation temperature, as can be seen by comparing the results in reference 17 with those in reference 18. The results contrary to the expectation in reference 19 may be caused by the imperfect fabrication and mounting in that work. Therefore, with

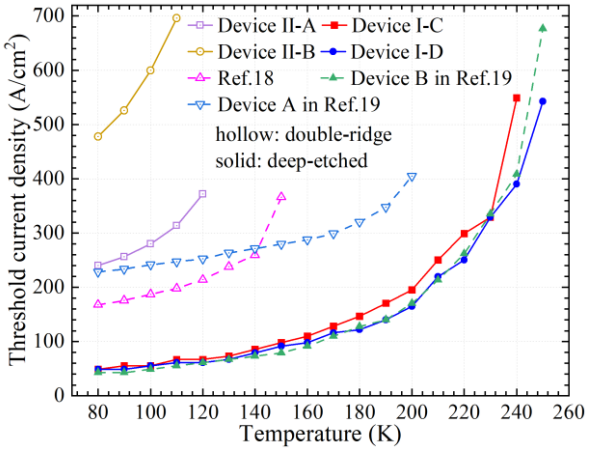

FIG. 3. Comparison of the CW threshold current densities for IC VCCLs from this work and previous work in references 18 and 19.

improved device fabrication using the double-ridge waveguide structure, it should be possible to achieve enhanced VCCL performance based on this type-I ICL wafer.

B. Spectral characteristics

Device II-A and the device in Ref. 18 have the same 8-μm-wide shallow-etched waveguide based on the same type-II ICL wafer; devices I-C, I-D and the deep-etched device B in Ref. 19 were processed from the same wafer V1080 with the same width of deep-etched waveguide. The main differences between the devices are the parameters of the half-wave couplers, L_C and w. As we described above, the normalized cross-coupling coefficient χ and relative phase, depending on the structural parameters of couplers, are important for tunability and high SMSR. Using the theoretical method in Ref. 15, the ideal normalized cross-coupling coefficient χ of all devices equals 0.02, and the values of χ and the relative phase calculated with the actual parameters of the couplers in Table I are shown in Table II, within their wavelength tuning range. As the lasing wavelength increases, the values of χ and relative phase change in a small range. The total tuning ranges and the maximums of the SMSR of every device are also listed in Table II.

Figure 4 displays the emission spectra of the type-II ICL devices employing the double ridge waveguide at different temperatures. Figure 5 shows the wavelength tuning and corresponding SMSR of the type-II ICL devices at different temperatures as a function of the injection current I_L. Device II-A operated with the tuning range of 8.21 nm, 15.68 nm, 14.13 nm, 53.35 nm and 55.23 nm at 82 K, 90 K, 95 K, 100 K and 110 K, respectively. A total 153.4-nm-wide wavelength tuning range could be obtained, over the range 3268.99 nm to 3422.43 nm, exceeding the previous result in Ref. 18 by 50%. The design parameters of device II-A obviously are closer to the ideal values in both χ and relative phase in the tuning range, which may contribute to

the wider tuning range compared with the device in Ref. 18. However, there is no significant improvement observed in SMSRs for device II-A (SMSRs of one-third of channels below 25 dB as shown in Fig. 5(a)) compared with that in Ref. 18 (over 25 dB in nearly all channels). This may be caused by the instability of the device process between different fabrication batches. The wavelength of device II-B could be tuned from 3263.81 nm to 3409.26 nm, with the temperature increasing from 82 K to 100 K. The tuning ranges were 74.94 nm and 69.19 nm at 82 K and 100 K, respectively. The channel interval of the two devices was approximately 1.74 nm at lower temperatures and slightly increased to 1.88 nm at higher temperatures. For device II-B, the coupler was designed close to the target and the device achieved a large tuning range of 145.45 nm with SMSRs mostly above 25 dB. The maximum measured SMSR was about 37 dB from device II-B at 82 K, which was limited by a finite dynamical range of the FTIR spectrometer. Similar observations were made for device A in Ref. 19, a type-I ICL device employing double-ridge waveguides. The coupler design closer to the ideal condition contributed to the excellent tuning range around 210 nm and the SMSRs of most channels varying from 25 dB to 35 dB.

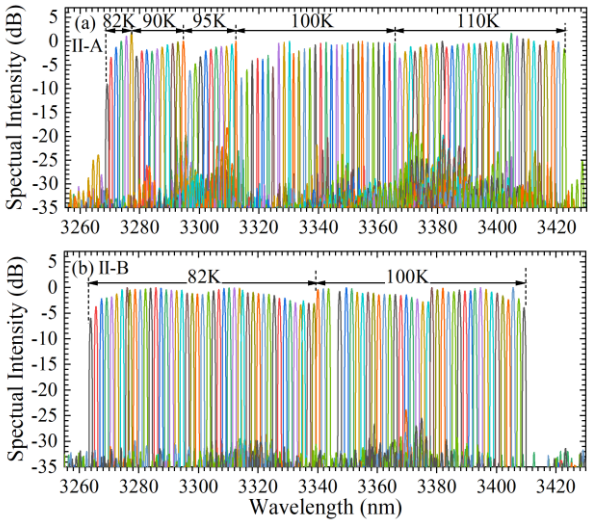

FIG. 4. Emission spectra of the V-coupled cavity ICLs with double ridge waveguide structure based on the type-II wafer: (a) device II-A and (b) device II-B.

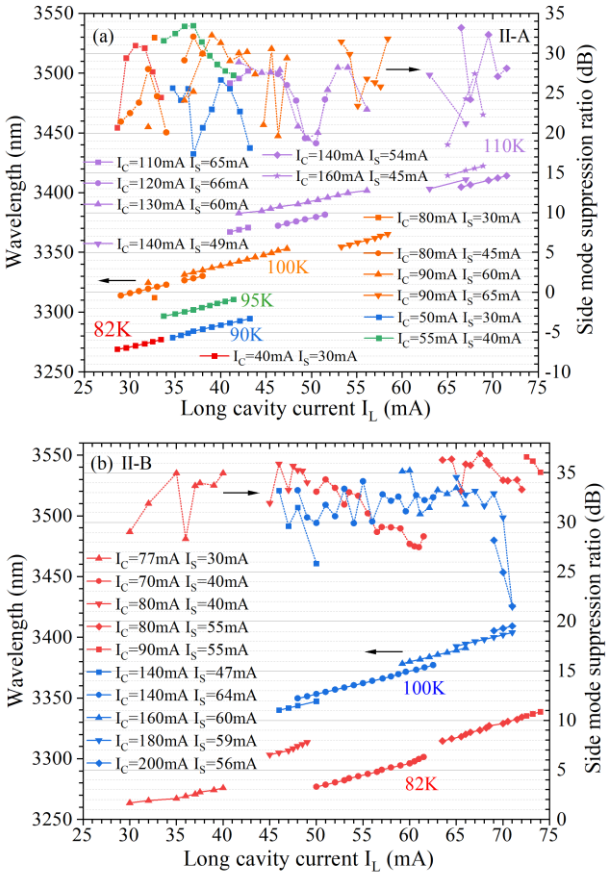

FIG. 5. The wavelength tuning and the corresponding SMSR of devices (a) II-A and (b) II-B against current I_L with various I_C and I_S. The long cavity current scans from 25 mA to 75 mA with the temperature varying.

The two type-I ICL devices with the deep-etched waveguide structure could be tuned at higher temperatures above 200 K and their overlapped emission spectra at different operating temperatures are shown in Figure 6. Device I-C delivered a consecutive wavelength tuning range of 67.9 nm, 17.8 nm, 20.2 nm and 29.8 nm at 205 K, 215 K, 225 K and 235 K, respectively. A total 138.9 nm wavelength tuning was demonstrated with a channel spacing of around 1.3 nm, varying from 2977.2 nm to 3116.1 nm. For device I-D, the wavelength of the main mode was tuned from 2999.4 nm to 3099.6 nm, covering a total of 77 channels, with the temperature increasing from 210 K to 240 K. The channel interval varied from 1.24 nm at 210 K to 1.32 nm at 240 K. Single-mode emission was observed at high temperatures up to

250 K, even though the continuous channel tuning was limited by insufficient thermal dissipation with a finite current range at heat-sink temperatures above 240 K. The wavelength tuning and corresponding SMSR of the type-I ICL devices at different temperatures as a function of the long cavity injection current is shown in Figure 7. According to the values of χ, device I-D and device B in Ref. 19, with the same 8-μm-wide deep-etched waveguide, are similar in theory and also exhibited similar tuning ranges and SMSRs. Although device I-C had a wider tuning range, its coupler design had a large deviation from the ideal value, especially at shorter wavelength, and may have caused the SMSRs of the channels near 2985 nm to be much lower than other channels and the absence of some channels at 205 K.

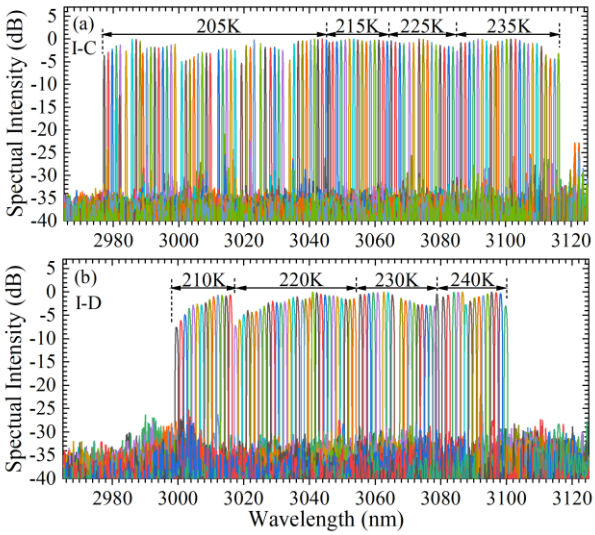

FIG. 6. Emission spectra of the V-coupled cavity ICLs with deep-etched waveguide structure based on the type-I wafer: (a) device I-C and (b) device I-D.

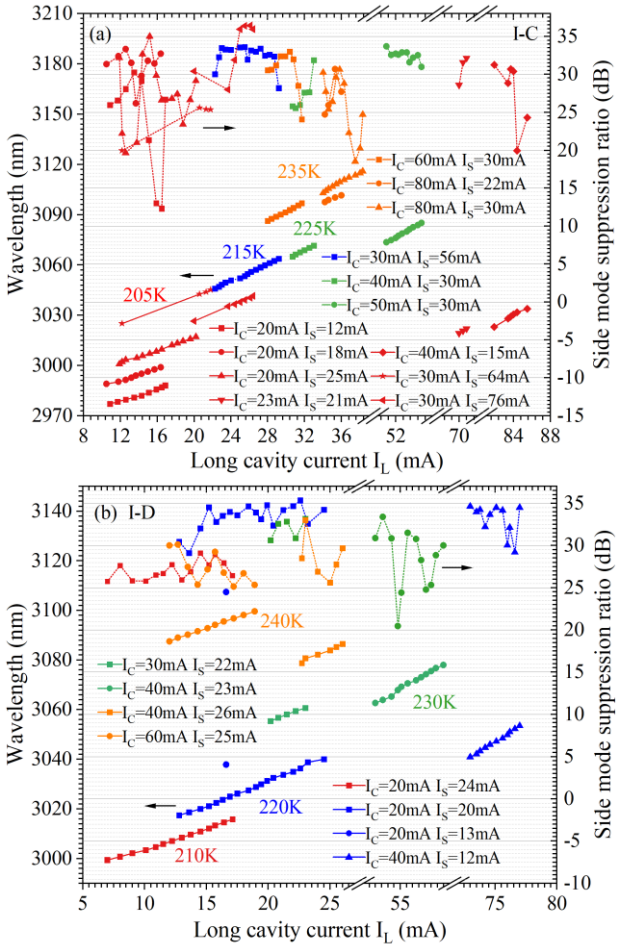

FIG. 7. The wavelength tuning and the corresponding SMSR of devices (a) I-C and (b) I-D against current I_L with various I_C and I_S. The long cavity current scans from 5 mA to 88 mA with temperature variations.

We conducted supplementary spectral measurements of device B in Ref. 19 at extended temperature range. The obtained emission spectra at 245 K and 250 K and the SMSR of each channel are shown in Fig. 8. At 245 K, device B in Ref. 19 achieved wavelength tuning of 33.9 nm from 3084.2 nm to 3118.1 nm, with a channel spacing of around 1.3 nm. The wavelength coverage at 245 K was limited by a finite current range and overlapped well with the tuning range in Ref. 19 at 240 K (from 3068 nm to 3117 nm), and the SMSRs of channels were also similar (varying between 25 dB and 35 dB). As the temperature rose to 250 K, a single-mode tuning range of 32.2 nm was still achievable and the operating wavelength was expanded to 3129.1 nm. The SMSRs of half of the channels were below 25 dB at 250 K. When the

operating temperature is close to or at the highest temperature of lasing, the SMSRs of channels would degrade due to limited thermal dissipation and a reduced current range that could be applied to under the increased temperature. Although the tuning range would be narrowed by the limited injection currents at the highest operating temperature for lasing, the observed tuning performance at 250 K confirmed that the VCCLs have a large potential for wider tuning with improved heat dissipation by electroplating thick Au layer or using more advanced ICL wafers.

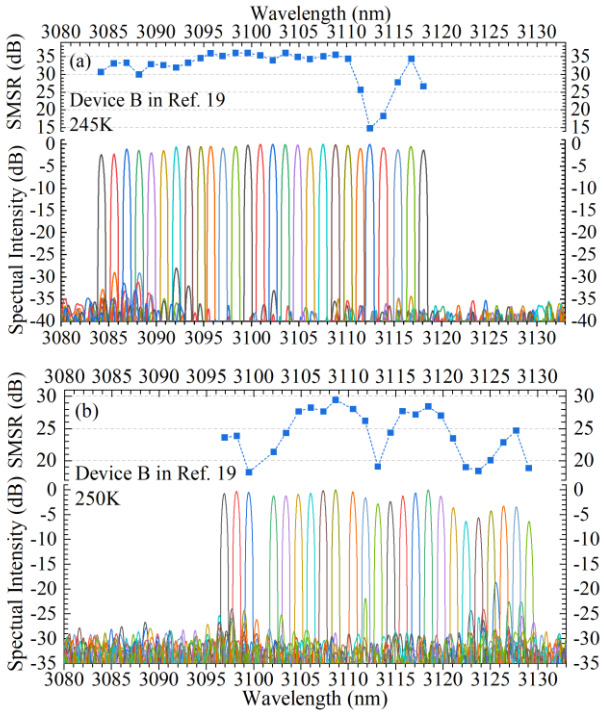

FIG. 8. Emission spectra of device B in reference 19 at (a) 245 K and (b) 250 K with the corresponding side mode suppression ratio (SMSR) of each channel.

As illustrated and discussed above, the devices with the ideal χ and the relative phase can have good performance in selecting modes and obtaining high SMSRs. Meanwhile, some devices, such as device I-C and the device in Ref. 18, with the design of couplers deviating from ideal values, can also work well in achieving single-mode emission with a wide wavelength tuning range exceeding 100 nm. The difference caused by the various coupler parameters between devices is not significant, when the values of L_C and w are varied within a certain range corresponding to the

deviation of χ and relative phase less than 0.01-0.015 and 20-30 degrees, respectively. For type-II ICL devices here, when the width of the shallow-etched waveguide is 8 μm (or 10 μm), the optimal value of w ranges from 6.2 μm to 6.7 μm (or 5.3 μm to 5.9 μm), the value of L_C varies from 68 μm to 79 μm (or 88 μm to 100 μm). As for type-I ICL devices with 8-μm-wide deeply-etched waveguides, the optimal value of w and L_C ranges from 1.5 μm to 2.2 μm and 38 μm to 50 μm, respectively. This indicates the good tolerance of the design and fabrication of the devices based on VCCL configuration.

IV. SUMMARY

We carefully investigated several single-mode tunable V-coupled ICLs based on two different wafers with different structures. It can be seen that all devices exhibit excellent tunability and prove that the V-coupled cavity lasers have a great potential for monolithically integrated widely tunable single-mode ICL lasers. The type-II ICLs with the double-ridge waveguide structure can be tuned a wavelength range of over 150 nm with temperatures varying from 82 K to 110 K. Additionally, the two type-I ICL devices exhibited excellent performance in wavelength tunability at higher temperatures above 200 K. One of the type-I ICLs with the deep-etched waveguide structure achieved a 138-nm-wide tuning range in the temperature range from 205 K to 235 K. The supplementary measurements for device B of Ref. 19 showed an expanded single-mode tuning at temperatures up to 250 K, suggesting the possibility of portable applications with a small-size thermal-electric cooler rather than liquid nitrogen cooling. These results were obtained for devices with various coupler parameters, demonstrating the good tolerance of the design and fabrication of VCCLs. Undoubtedly, there is still room for further improvement of the monolithic integrated V-coupled cavity ICLs for higher operating temperatures and wider tuning ability.

This is verified by comparison between devices made from the type-II and type-I ICL wafers with different threshold characteristics and temperature performance. Compared to the type-II ICLs studied in this work, the type-I ICLs had much lower threshold current density and consequently they were able to operate in cw mode in a wider temperature range and with a wide allowable current range to achieve widely-tunable single-mode operation. Hence, it is expected that a wider tuning range of single-mode mid-IR VCCLs will be achieved at room temperature and above with the use of the state-of-the-art type-II ICL wafers, which can have further lower threshold current densities in a wide temperature range.

ACKNOWLEDGMENTS

The work at Zhejiang University was supported by the National Natural Science Foundation of China (61960206001 and 62027825). The work at University of Oklahoma was partially supported by NSF (No. ECCS-1931193) and The Oklahoma Center for the Advancement of Science and Technology (OCAST) (AR21-024).

AUTHOR DECLARATIONS

Conflict of Interest

The authors have no conflicts to disclose.

DATA AVAILABILITY

The data that support the findings of this study are available from the corresponding author upon reasonable request.

REFERENCES

[1]R. Q. Yang, poster P3.80 at *7th Inter. Conf. on Superlattices, Microstructures and Microdevices*, Banff, Canada, 22-26 August 1994; Superlattice. Microst. **17**, 77 (1995).

[2]C. H. Lin, R. Q. Yang, D. Zhang, S. J. Murry, S. S. Pei, A. A. Allerman, and S. R. Kutz, Electron. Lett. **33**, 598 (1997).

[3]I. Vurgaftman, W. W. Bewley, C. L. Canedy, C. S. Kim, M. Kim, C. D. Merritt, J. Abell, J. R. Lindle, and J. R. Meyer, Nat Commun. **2**, 585 (2011).

[4]R. Q. Yang, L. Li, W. X. Huang, S. M. S. Rassel, J. A. Gupta, A. Bezinger, X. H. Wu, G. Razavipour, and G. C. Aers, IEEE J. Sel. Top. Quant. **25**, 1200108 (2019).

[5]J. R. Meyer, W. W. Bewley, C. L. Canedy, C. Kim, M. Kim, C. Merritt, and I. Vurgaftman, Photonics-basel **7**, 75 (2020).

[6]J. Nauschütz, H. Knotig, R. Weih, J. Scheuermann, J. Koeth, S. Hofling, and B. Schwarz, Laser Photonics Rev. **17**, 2200587 (2023).

[7]Y. Shen, J. A. Massengale, R. Q. Yang, S. D. Hawkins, and A. J. Muhowski, Appl. Phys. Lett. **123**, 041108 (2023).

[8]R. Q. Yang, C. J. Hill, K. Mansour, Y. M. Qiu, A. Soibel, R. E. Muller, and P. M. Echternach, IEEE J. Sel. Top. Quant. **13**, 1074 (2007).

[9]C. S. Kim, M. Kim, J. Abell, W. W. Bewley, C. D. Merritt, C. L. Canedy, I. Vurgaftman, and J. R. Meyer, Appl. Phys. Lett. **101**, 061104 (2012).

[10]J. Scheuermann, R. Weih, M. von Edlinger, L. Naehle, M. Fischer, J. Korth, M. Kamp, and S. Höfling, Appl. Phys. Lett. **106**, 161103 (2015).

[11]J. Nauschütz, J. Scheuermann, R. Weih, J. Koeth, B. Schwarz, and S. Höfling, Electron. Lett. **59**, e12968 (2023).

[12]X. Feng, M. Stocker, J. Pham, F. Towner, K. Shen, J. Wang, and K. Lascola, Appl. Phys. Lett. **112**, 131102 (2018).

[13]D. Caffey, T. Day, C. S. Kim, M. Kim, I. Vurgaftman, W. W. Bewley, J. R. Lindle, C. L. Canedy, J. Abell, and J. R. Meyer, Opt. Express **18**, 15691 (2010).

[14]E. Giraud, P. Demolon, T. Gresch, L. Urio, A. Muller, and R. Maulini, Opt. Express **29**, 38291 (2021).

[15]J. J. He, and D. Liu, Opt. Express **16**, 3896 (2008).

[16]S. Zhang, J. J. Meng, S. L. Guo, L. Wang, and J. J. He, Opt. Express **21**, 13564 (2013).

[17]H. T. Yang, R. Q. Yang, J. L. Gong, and J. J. He, Opt. Lett. **45**, 2700 (2020).

[18]J. L. Gong, R. Q. Yang, Z. Y. Wang, and J. J. He, IEEE Photonic. Tech. L. **35**, 309 (2023).

[19]J. L. Gong, Z. Y. Wang, J. J. He, L. Li, R. Q. Yang, and J. A. Gupta, Opt. Express **31**, 38409 (2023).

[20]L. Esaki, L. L. Chang, and E. E. Mendez. Jpn. J. Appl. Phys. **20**, L529 (1981).

[21]J. R. Meyer, C. A. Hoffman, F. J. Bartoli, and L. R. Rammohan, Appl. Phys. Lett. **67**, 757 (1995).

[22]R. Q. Yang, "Interband Cascade (IC) Lasers", in *Semiconductor lasers: fundamentals and applications*, edited by A. Baranov and E. Tournie (Woodhead Publishing Limited, Cambridge, UK, 2013), Chap. 12.

[23]L. Shterengas, R. Liang, G. Kipshidze, T. Hosoda, S. Suchalkin, and G. Belenky, Appl. Phys. Lett. **103**, 121108 (2013).

[24]Y. C. Jiang, L. Li, R. Q. Yang, J. A. Gupta, G. C. Aers, E. Dupont, J. M. Baribeau, X. H. Wu, and M. B. Johnson, Appl. Phys. Lett. **106**, 041117 (2015).

[25]L. Shterengas, G. Kipshidze, T. Hosoda, R. Liang, T. Feng, M. Wang, A. Stein, and G. Belenky, IEEE J. Sel. Top. Quant. **23**, 1500708 (2017).

[26]C. Borgentun, C. Frez, R. M. Briggs, M. Fradet, and S. Forouhar, Opt. Express **23**, 2446 (2015).

TABLES

TABLE I. The structural parameters of different IC VCCLs analyzed in this work. The VCCLs were made by type-I and type-II ICL wafers and employed deep-etched or double-ridge waveguide structures.

Parameters	Type-II ICLs			Type-I ICLs			
	REF. 18	II-A	II-B	I-C	I-D	REF. 19 Device A	REF. 19 Device B
Shallow-etched waveguide width (μm)	8	8	10	/	/	6	/
Deep-etched waveguide width (μm)	18	23	15	8	8	21	8
Coupler gap w (μm)	5.1	6.4	5.3	2.1	1.7	4.9	2.2
Coupler length L_C (μm)	76	70	100	38	39	62	44

TABLE II. Achieved tuning performance of the ICLs and the values of normalized cross-coupling coefficient χ and the relative phase calculated with the parameters of the couplers, corresponding to the tuning range of the devices.

Device	Tuning range	Maximum of SMSR (dB)	Normalized cross-coupling coefficient χ	Relative phase (degree)
REF. 18	3329.9 nm to 3431.3 nm	35.7	0.045 to 0.048	155 to 151
II-A	3269.0 nm to 3422.4 nm	33.4	0.011 to 0.013	181 to 178
II-B	3263.8 nm to 3409.2 nm	36.9	0.018 to 0.024	177 to 172
I-C	2977.2 nm to 3116.1 nm	36.4	0.005 to 0.007	155 to 160
I-D	2999.4 nm to 3099.6 nm	35.3	0.007 to 0.011	172 to 173
REF. 19 Device A	2845.5 nm to 3055.5 nm	34.4	0.011 to 0.018	164 to 199
REF. 19 Device B	2997.6 nm to 3117.5 nm (Expand to 3129.1 nm at 250 K)	36	0.009 to 0.013	157 to 159

FIGURE CAPTIONS

FIG. 1. The schematic drawing of the cross-sectional view of (a) the double-ridge waveguide based on type-II ICL wafer and (b) the deep-etched waveguide based on type-I ICL wafer. (c) The schematic drawing of a V-coupled cavity laser.

FIG. 2. Electrical and optical characteristics of IC VCCLs at different temperatures. Devices (a) II-A and (b) II-B: the long cavity current is 40 mA and the short cavity current is 30 mA; devices (c) I-C and (d) I-D: the long cavity current and the short cavity current are both 30 mA.

FIG. 3. Comparison of the CW threshold current densities for IC VCCLs from this work and previous work in references 18 and 19.

FIG. 4. Emission spectra of the V-coupled cavity ICLs with double ridge waveguide structure based on the type-II wafer: (a) device II-A and (b) device II-B.

FIG. 5. The wavelength tuning and the corresponding SMSR of devices (a) II-A and (b) II-B against current I_L with various I_C and I_S. The long cavity current scans from 25 mA to 75 mA with the temperature varying.

FIG. 6. Emission spectra of the V-coupled cavity ICLs with deep-etched waveguide structure based on the type-I wafer: (a) device I-C and (b) device I-D.

FIG. 7. The wavelength tuning and the corresponding SMSR of devices (a) I-C and (b) I-D against current I_L with various I_C and I_S. The long cavity current scans from 5 mA to 88 mA with temperature variations.

FIG. 8. Emission spectra of device B in reference 19 at (a) 245 K and (b) 250 K with the corresponding side mode suppression ratio (SMSR) of each channel.